Transition Mixing Ratios Determined from a Study of the Electron and Gamma-Ray Distributions from Oriented ^{192}Ir

Alan T. Hirshfeld and Dale D. Hoppes
National Bureau of Standards, Washington, D. C. 20234
(Received 23 July 1970)

The angular distributions measured for 12 γ rays in ^{192}Os and ^{192}Pt resulting from the decay of cryogenically oriented ^{192}Ir have been used to determine the following $E2/M1$ mixing ratios: 201 keV, $\delta^2 > 3.7$; 296 keV, $\delta = -(6^{+3}_{-1})$; 308 keV, $\delta = -(7.1 \pm 0.6)$; 417 keV, $\delta = 4^{+7}_{-3}$; 485 keV, $\delta = 5.8 \pm 0.8$; 604 keV, $\delta = 1.5 \pm 0.1$, following the Rose-Brink sign convention. The angular distribution of the 672-keV β group and the above γ measurements limit the relative contribution, I_L, of different operator tensor ranks, L, involved in each β transition. The results for electron-capture transitions terminating at levels in osmium are: 694-keV level, $I_1 > 0.9$; 584-keV level, $I_0 > 0.6$, $I_2 < 0.1$. For β transitions feeding platinum states, we determine: 921-keV level, $I_1 > 0.8$; 785-keV level, $I_1 > 0.92$, $I_2 < 0.03$. The ^{192}Ir ground-state magnetic moment is determined to be positive.

1. INTRODUCTION

The decay of the 74-day ground state of ^{192}Ir (Fig. 1) has intrigued many recent investigators.[1-8] Measurements and theoretical calculations[9] of energies, moments, and transition probabilities for the resultant osmium and platinum nuclei have demonstrated the differing natures of states of the same spin in the two daughters.

Our goals in the present study were threefold. The γ-ray $E2/M1$ mixing ratios had not been well established at the time the present experiments were initiated. A report[10] of an unusual 536-keV β-γ angular correlation suggested that a study of the β distributions from oriented nuclei might prove interesting. The determination of these distributions for a spectrum rich in conversion electrons was considered an interesting test of techniques for quantitative electron spectroscopy of nuclei cryogenically oriented in ferromagnetic foils.

The presentation of accurate γ-ray distribution results by an Oxford group[11] while our work was in progress enabled us to bypass a determination of the hyperfine interaction and deduce our orientation parameters directly from the measured distribution for the 468-keV γ ray. We supplement their measurement of the magnitude of the ^{192}Ir ground-state magnetic moment by establishing the sign.

2. DESCRIPTION OF THE EXPERIMENT

A measured angular distribution of radiation can be described by

$$W(\theta) = 1 + \sum_{n=1} A_n Q_n P_n(\cos\theta),$$

where the observed intensity is normalized to the isotropic radiation observed with the nuclei unoriented. In our case the θ appearing in the Legendre-polynomial argument is measured between the resultant magnetic field direction in a thin iron foil and the detection direction. The Q_n are known corrections for the finite angular extent of the detectors. Each A_n, which is then determined by sampling the distribution at sufficient angles to separate the contribution of different P_n terms, can be further decomposed into factors depending on the orientation of the initial state, the reorientation due to the angular momentum carried away by any intervening transition, and a distribution parameter characteristic of spins and operators involved in the transition actually observed.

γ-ray distributions. For these we adopt the formalism of Rose and Brink[12] where a decay $J_1 \xrightarrow{L_{12}} J_2 \xrightarrow[L,L']{} J_3$, with orientation of the initial state and observation of the γ-ray transition from J_2 to J_3, is described by

$$A_n = B_n(J_1) U_n(J_1 J_2) R_n(J_2 J_3).$$

The orientation parameter

$$B_n(J) = \sum_M w(M)(-)^{J-M}(2J+1)^{1/2}(JJM - M|n0)$$

gives the initial orientation in terms of the relative populations, $w(M)$, of the magnetic substates of J and a coupling coefficient reflecting the moment being described. The repopulation coefficient, $U_n(J_1 J_2)$, is an intensity-weighted average of the tabulated quantities $U_n(L_{12} J_1 J_2)$ describing the change in the orientation after a transition via operators of various tensor ranks, L_{12}. No interference terms between different tensor ranks (or equivalently, different multipolarities) occur. Successive unobserved transitions are represented by a product of the repopulation coefficients corre-

sponding to each transition; parallel feedings again give a weighted average.

The distribution parameters, $R_n(J_2J_3)$, depend directly on the ratio of the reduced matrix-element amplitudes for the two possible operators contributing to the observed γ transition. Explicitly, here

$$R_n=\frac{R_n(\bar{L}\bar{L}J_2J_3)+2\delta R_n(\bar{L}LJ_2J_3)+\delta^2R_n(LLJ_2J_3)}{1+\delta^2}.$$

The $R_n(LL'J_2J_3)$ are tabulated combinations of vector coupling coefficients for multipolarities L and $\bar{L}$, where $\bar{L}$ is the smaller. The mixing ratio

$$\delta=\frac{\langle J_2\|\vec{T}_L^{\langle\pi\rangle}\|J_3\rangle(2L+1)^{-1/2}}{\langle J_2\|\vec{T}_{\bar{L}}^{\langle\pi\rangle}\|J_3\rangle(2\bar{L}+1)^{-1/2}}$$

is so defined as to be independent of the experiment in which it is determined. The label $\langle\pi\rangle$ only indicates that the operator is known to be electric or magnetic in nature; the γ distribution does not show explicitly whether the parity changes in the transition. Since δ^2 is the ratio of intensities due to the two operators, it is also (when normalized) the weighting factor used in calculating the repopulation coefficients appearing in the distribution for a subsequent γ ray.

Experimentally, two γ-ray detectors suffice for a simultaneous determination of the full distribution, for only A_2 and A_4 should be nonzero in the present case. The counting rate at each temperature for detectors at $\theta=0$ and $\theta=\pi/2$ is normalized to the corresponding rate seen at a sample temperature sufficiently high to destroy any orientation.

β-ray distributions. Here we will use the early formulation of Morita and Morita[13] adapted to the present terminology. As before, Q_n and P_n are given quantities and A_n is to be determined. In this case $A_n=B_n(J_1)R_n(J_1J_2)$, since the transitions proceed directly from the initial oriented state. The orientation parameters are defined as before, but the distribution parameters are much more complex. A number of operators are possible, grouped into three different tensor ranks, for the present first-forbidden β decay. Moreover, each bilinear product is multiplied by a product of energy-dependent electron wave functions. These combinations are collected in the particle parameters, $b_{LL'}^{(n)}$, of Ref. 13. Retaining the matrix-element definition (up to a factor i) of that reference, we can then write the distribution parameters as

$$R_n(J_1J_2)=\frac{\sum_{L\geq L'}(-)^{L+L'+n}W(J_1J_1LL';nJ_2)b_{LL'}^{(n)}}{\sum_L W(J_1J_1LL;0J_2)b_{LL}^{(0)}}.$$

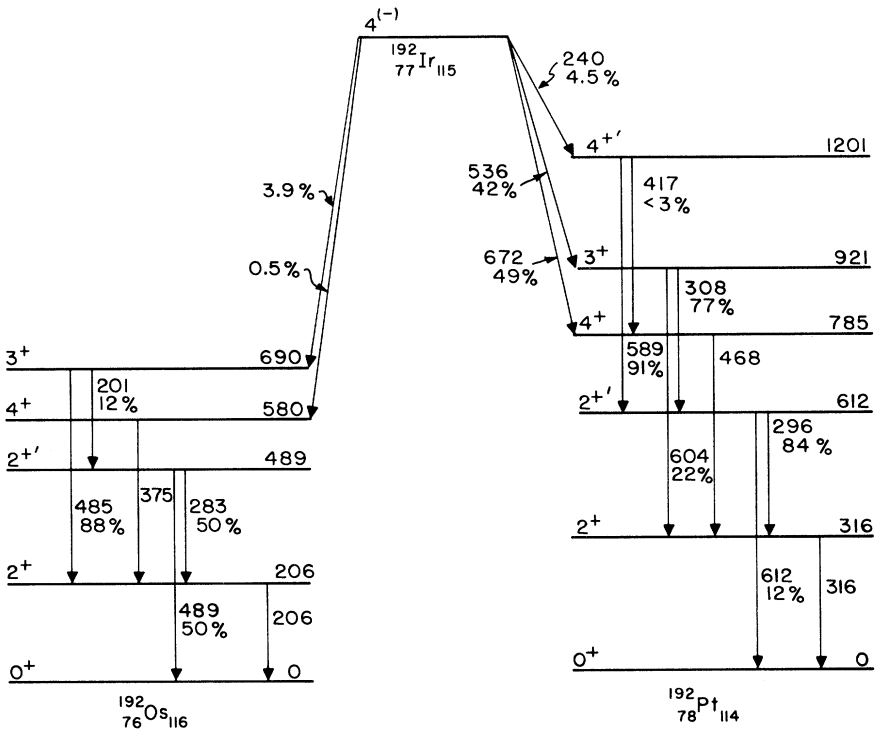

FIG. 1. The pertinent features of the decay scheme of ^{192}Ir, as taken from *Tables of Isotopes*, by C. M. Lederer, J. M. Hollander, and I. Perlman (John Wiley & Sons, Inc., New York, 1967).

We shall see that for our data a simple analysis based on a crude approximation will suffice. This is given in Appendix 2 of Ref. 13 and is based on using only the leading terms in a Coulomb wave-function expansion for the outgoing electron and on the assumption that the tensor rank-two matrix element might play a relatively important role. It uses a grouping of the reduced matrix elements of the (in general) six operators according to tensor rank to form three new parameters: $\lambda = VC_A M(i\vec{\sigma}\cdot\vec{r}) - C_A M(\gamma_5)$ for tensor rank zero; $\mu = VC_v M(i\vec{r}) - C_v M(\vec{\alpha}) + VC_A M(\vec{\sigma}\times\vec{r})$ for rank one: and $= C_A M(iB_{ij})$ for tensor rank two. V is the Coulomb factor $\alpha Z/2\rho$, and the matrix elements are real. The particle parameters are then simple combinations of λ, μ, and ν with analytic energy-dependent factors. For example, the denominator of $R_n(J_1 J_2)$ displayed above becomes $2[\lambda^2+\mu^2+\frac{1}{12}(K^2+p^2)\nu^2]$, where K and p are the momenta of the neutrino and electron, respectively. This denominator is also the "shape factor" showing the deviation of a spectrum from that for an allowed decay, while the integral of each term over energy represents the relative transition probability for each tensor rank. The latter quantities (λ^2, μ^2, and approximately $0.18\nu^2$) are the weight factors to be used for determining the repopulation factors applicable to the distribution of subsequent radiation.

In general P_1, P_2, and P_3 terms appear in the β distribution, but space considerations in our apparatus permit only one β detector. Even so, the P_2 contribution can be separated from the odd terms, since it remains the same when the polarizing field is reversed at constant temperature. The anticipated relative size of the P_3 term suggests that it can be neglected unless A_2 is large. Thus the β-distribution parameters R_1 and R_2 can be obtained at each energy directly from the normalized counting rates for two field directions and the orientation parameters determined from a known γ distribution monitored simultaneously. These distribution parameters are then to be compared with those computed as functions of ratios of λ, μ, and ν. These ratios must also yield the values of the repopulation coefficients observed in γ-ray transitions following the β decay.

3. DESCRIPTION OF THE APPARATUS AND TECHNIQUE

The foil samples were cooled by adiabatic demagnetization in a cryostat shown schematically in Fig. 2. The sample space shown was surrounded by a tailed Dewar system to allow a close approach of the γ detectors. The heat of magnetization of the chromium potassium alum cooling pill was carried off to the pumped ^{3}He bath by raising the sample assembly to contact the copper heat conductor. Susceptibility coils monitored the salt temperature and most significantly were used to insure that a temperature greater than 2 K was achieved for the warm normalizing counts. Further details of the apparatus will be reserved for a later paper. Some particular aspects of sample preparation and problems of adequate spectroscopy will be discussed here.

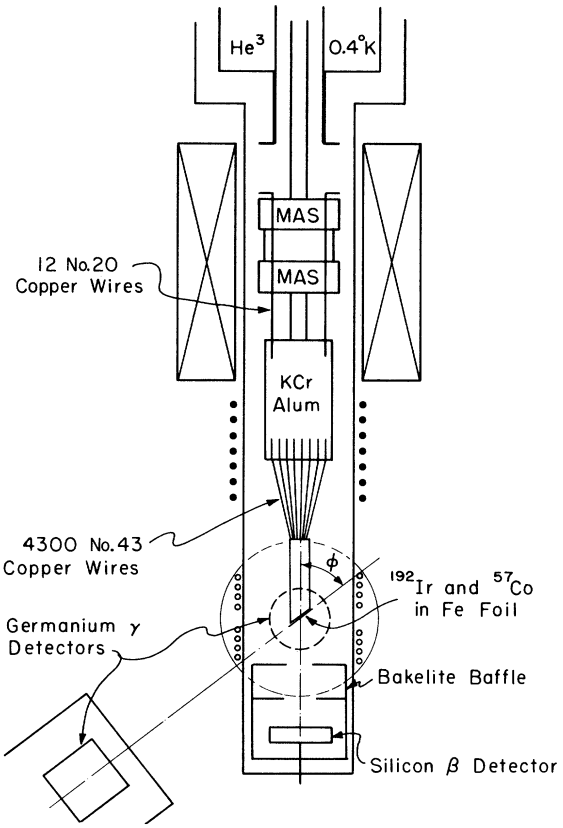

FIG. 2. Experimental apparatus. Shown surrounding the sample space are the 20-kOe superconducting solenoid, the susceptibility coil pair, and the 3-kOe (max) polarizing coils.

Sample preparation. Early experiments showed that iridium atoms present in dilute concentrations in an annealed bulk-iron sample experience a large effective magnetic field at the nucleus.[14,15] For successful electron spectroscopy our sources had to be thin; ideally a minimum number of mass-192 nuclei would have been implanted with an isotope separator. This was not possible at the time, so we attempted to produce such sources by controlled diffusion of moderately high specific activity ^{192}Ir (2 μCi/g Ir) into 1-mil iron foils. Preliminary runs with weak (1 μCi) sources plated onto a 2-mm-diam region of the foils and heated for 10 min at 1100°C in an argon atmosphere showed large an-

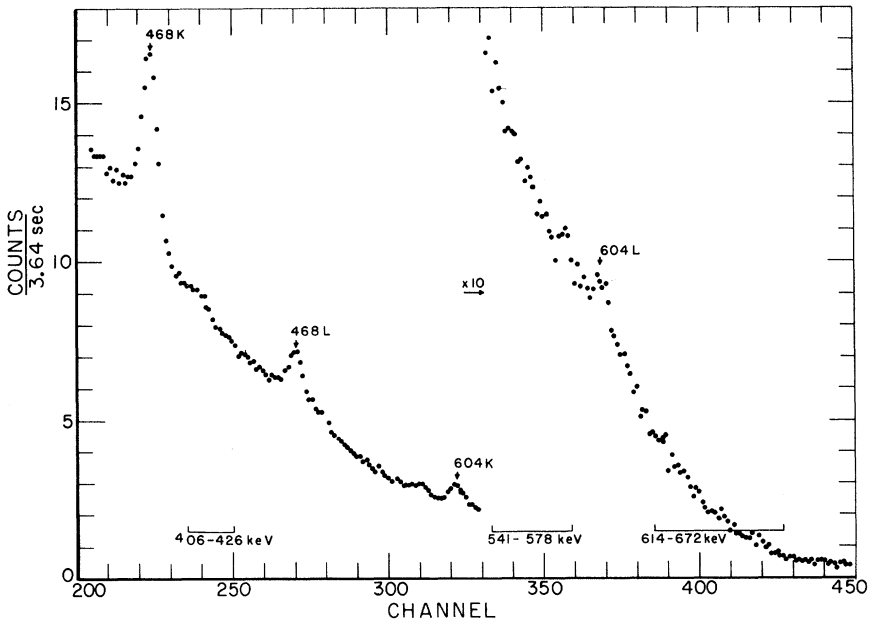

FIG. 3. The higher-energy half of the electron spectrum of ^{192}Ir, showing regions selected for analysis. This is a 64-min isotropic sampling taken during an orientation experiment. The polarizing field was 1 kOe.

isotropies. For a polar counter the counting rate doubled for the 604-keV γ ray when the temperature was reduced to 13 mK. The conversion-electron peaks were almost identical with those taken with a thin source when viewed with our system [resolution of 5 keV full width at half maximum (FWHM) at 390 keV].

However, sources intense enough (15 μCi) to permit reasonable counting rates for the weaker γ rays produced much smaller anisotropies at a given temperature (determined from the angular distribution of the 136-keV γ ray from 30 μCi of ^{57}Co previously diffused into the same foil and counted simultaneously). They also showed a much slower saturation of the anisotropy with increasing external polarizing field (600 to 2500 Oe). The strong field dependence persisted even when source diameters of 1 cm were used and the diffusion time was increased to 30 min. This diffusion produced a broadening of the conversion-electron peaks considered the maximum compatible with good spectroscopy at the energies under consideration (200–700 keV).

β detectors. The β detector was either a commercial silicon surface-barrier detector on a 1-mm-thick wafer or a National Bureau of Standards–prepared surface barrier on a p-type silicon disk 3 mm thick. Both types deplete fully at 1.5 K and are capable of operating with sufficient stability and resolution. They did not always do so on consecutive runs, however, and this resulted in rejection of some of the electron data. The β preamplifier head was also operated at 1.5 K. A spectrum taken during an orientation run is shown in Fig. 3.

The high fields necessary to produce maximum orientation led to an uncertainty in the electron counting. The apparatus shown in Fig. 2 utilized a magnetic field parallel to a line connecting the source and detector centers, if the distortion due to the foil is neglected. This arrangement should not have changed the average observation angle, but the spiralling of the electrons did produce an energy-dependent solid angle. At 485 keV a 2-kOe field produced a 22% increase in counting rate for the dimensions used. Since the normalizing isotropic count was taken under the same conditions, this led to only a small correction. However, the influence on very low-energy electrons was much stronger; the possibility of summing with coincident conversion electrons was large and could be gauged by the reduction in the area of the K conversion peaks of the 316-keV transition relative to the β spectrum at its base. A 0.55-mg/cm^2 plastic film placed over the detector to protect its surface from contaminants rejected tightly spiralling very low-energy electrons with little effect on those of interest.

Electron scattering from the stainless-steel experimental chamber walls, while adding less than 1% to high-energy conversion-electron-peak counts, would have added twice the total peak count distributed over lower energies. A plastic liner (tolerable in our cryostat where exchange

gas is not used to carry away the heat of magnetization) reduced this by half and shifted the distribution to lower energies; antiscattering baffles almost eliminated the remainder.

Electron scattering from the foil could not be so simply reduced. With a 16° angle subtended by the detector radius at the source, a foil angle, ϕ, of 20° produced five times the number of scattered electrons that a 40° angle did. The observed spectral distribution for scattering of 975-keV ^{207}Bi conversion electrons rose from near zero at low energies to a maximum not far below the original energy. Again a higher-energy conversion-peak area is not detectably affected by the scattering.

For most of the experimental runs the detector was collimated to a 9° half angle and a foil angle between 35 and 40° was used. Under these conditions the total scattered contribution was minimized, while $P_2(\cos\theta)$ was 0.4. The apparent (zero field) Q_1 and Q_2 were always greater than 0.98.

γ detectors. The two Ge(Li) detectors used for the γ data reported here were approximately the same in their response at 1.33 MeV: resolution better than 2.5 keV FWHM and greater than 3% peak efficiency relative to a 3-in.×3-in. NaI detector at 25 cm. The 0 and $\pi/2$ detector distances (source center to Ge sensitive face) were, respectively, 14.3 and 8.5 cm, corresponding to $Q_2 = 0.988$, $Q_4 = 0.962$ and $Q_2 = 0.979$, $Q_4 = 0.942$. Coincident summing of the more intense lower γ rays was calculated to contribute less than 0.3% to their corresponding crossover transitions.

The relatively good γ-ray resolution was important not only for the clear separation of close-spaced γ rays (Fig. 4) but also to allow rejection of the (anisotropic) scattered radiation. The cryostat was designed to minimize scattering, but the polar detector still displays a flat region below a 279-keV peak about twice as high for a ^{203}Hg source in the experimental position as for the same source in free space.

Gain stability for the γ detectors over the 5- or 6-h counting period after each demagnetization was usually satisfactory for an integrated-peak evaluation, although a channel-by-channel comparison of the counts for the nuclei oriented and unoriented often revealed fractional channel shifts for each detector.

No unusual features were utilized in the remainder of the spectroscopic equipment. The output of each of the three detectors was recorded in a separate 400- or 512-channel analyzer. The limited number of channels and the small separation of the γ energies did not permit us to examine the regions above 625 keV in the γ spectra. Analyzer dead times were less than 15% for the γ systems and usually less than 20% for the β, where baseline restoration made a significant improvement in resolution.

4. DATA AND ANALYSIS

The early runs with weak sources suffer from poor statistics, the use of only one γ detector, or poor temperature determinations. The γ-ray data actually used in this analysis covered a range of 2.4 in the orientation parameter B_2, but did not include the lower-temperature region which would give large B_4 values and accentuate the P_4 terms. These terms are significant for firmly establishing the hyperfine interaction and deciding the tensor rank of the operators responsible for intervening transitions. Since the first point is already beclouded by the peculiarities of our source, we do not attempt to make a determination of the hyperfine interaction. However, the limitation on the accuracy for the U_4's does increase our error limits for the transitions in which no direct observations are possible.

Twelve γ rays resulting from the ^{192}Ir decay were analyzed, as were the two γ rays of ^{57}Co used to confirm the detector angles and establish the foil temperature. The peaks that were well separated from the others were treated by summation of counts over all channels generously spanning the apparent peak, after subtraction of a background determined by graphical (nonlinear) extrapolation from slightly higher channels.

The 296-, 308-, and 316-keV peaks were analyzed by fitting monoenergetic response functions determined under the same experimental conditions in order to adjust for the contribution of low-energy portions of higher-energy peaks. This contribution was quite large (over 20% of the true peak in some cases) due to the accentuated scattering from the cryostat materials. A similar treatment was applied to the 589-, 604-, and 612-keV complex, but the diminishing intensity with increasing energy made such an approach unnecessary for the 468-, 485-, and 489-keV group.

Average values of A_2 and A_4 were determined for each peak for each of 10 different temperature intervals. The orientation parameters B_2 and B_4 were then derived for each temperature from the A_2 measured for the 468-keV γ ray, using the relations $B_2 = A_2/-0.381$ and $\mu H = 1.08\times10^{-24}$ J, as reported in Ref. 11.

The average U_2R_2 and U_4R_4 for each γ ray were then calculated from these values, using the B_2 and B_4 for each period as weighting factors. The resultant values for the U_2R_2's are displayed in Fig. 5, where the error bars represent the standard error of the mean for the 10 samplings. This error includes not only counting statistics, but also contributions due to possible inapplicability of

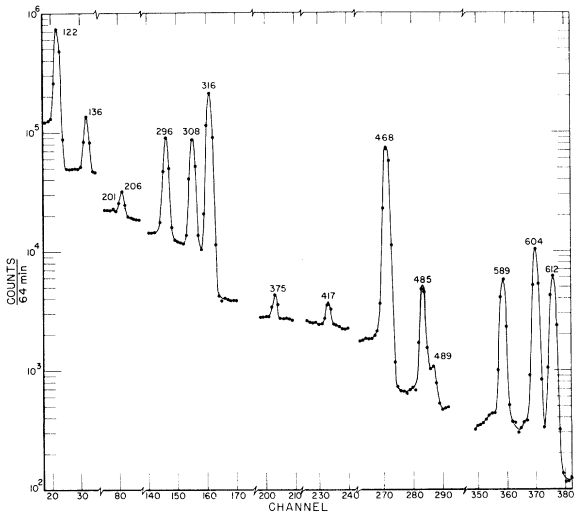

FIG. 4. The γ-ray spectrum of ^{192}Ir plus ^{57}Co recorded along the orientation axis. This is an isotropic sampling of 64-min duration. The spectrum collected by a detector placed perpendicular to the orientation axis had less scattered radiation and three times the counting rate.

the hyperfine value used and any time- or temperature-dependent fluctuations. Seven of the γ rays are pure $E2$; for these the influence of the preceding radiations is exhibited by also plotting the unattenuated $E2$-distribution coefficient. Values reported in Ref. 11 for the stronger transitions are also shown; the agreement is excellent for all except the 612 keV and the 296 keV, where the different treatment of the background may contribute to the discrepancy.

The procedure for determining the individual repopulation coefficients and distribution parameters is as follows: The γ-ray distribution for the transitions from the top level in each daughter is considered first. For pure $E2$ transitions, where R_2 and R_4 are known, the U_2 and U_4 due to the preceding β decay are directly evaluated and applied (along with U's due to the $E2$ transition) to the analysis of subsequent transitions. If the initial γ-ray mixture is not known, an approximate mixing evaluation fitting both the U_2R_2 and U_4R_4 terms is used for approximate repopulation coefficients to be applied to a subsequent $E2$ γ ray. The distribution of the $E2$ γ is then used to correct or affirm the initial determination of the repopulation coefficients due to the β transition and so on down to the lowest excited state. In the case of the 489-keV transition in ^{192}Os the γ distribution is used to evaluate the mixing in the preceding 201-keV γ transition, which was too weak relative to its background to measure directly.

Our γ-mixing results are displayed in Table I, along with values from other sources. Previous arguments and measurements[3-5] have been used to eliminate alternate choices that were sometimes possible. The errors are those propagated from the standard error of the mean shown in Fig. 5; in some cases the uncertainty in the repopulation coefficients has considerably increased the error for δ. Also, doubling the error on R_n would in some cases permit other regions of δ to be admissible, as is illustrated in Ref. 4.

The use of the repopulation coefficients determined in the above analysis to limit the β-decay matrix elements in the $4^- \rightarrow 4^+$ transitions does not always produce clear-cut results if the possibility of a tensor rank-two operator, B_{ij}, is admitted. For example, the U_2 and U_4 due to the 672-keV β group fit quite well pure tensor rank-one operator, and this fact was used in Ref. 11 to limit the tensor rank-zero contribution, while neglecting the B_{ij} contribution. If all contributions are included,

$$U_2 = \frac{\lambda^2 + 0.850\mu^2 + 0.103\nu^2}{\lambda^2 + \mu^2 + 0.18\nu^2} ,$$

$$U_4 = \frac{\lambda^2 + 0.500\mu^2 - 0.027\nu^2}{\lambda^2 + \mu^2 + 0.18\nu^2} .$$

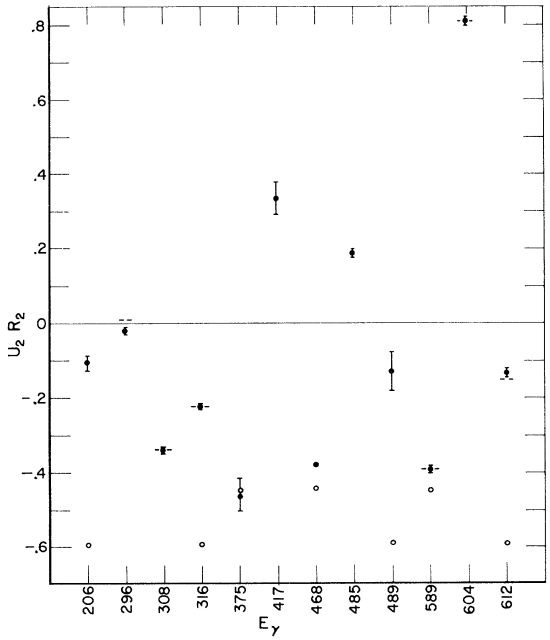

FIG. 5. A display of the product of the repopulation coefficient and the distribution parameter measured for 12 γ rays resulting from the decay of ^{192}Ir. Our values are shown as solid dots with vertical flags giving the standard error of the mean for 10 measurements at different temperatures. The horizontal dashes show the values reported in Ref. 11. The open circles show the unattenuated distribution parameter for seven $E2$ transitions.

TABLE I. γ-ray mixing ratios, δ.

Method and reference	201 keV $3^+ \rightarrow 2^{+\prime}$ Os	296 keV $2^{+\prime} \rightarrow 2^+$ Pt	308 keV $3^+ \rightarrow 2^{+\prime}$ Pt	417 keV $4^{+\prime} \rightarrow 4^+$ Pt	485 keV $3^+ \rightarrow 2^+$ Os	604 keV $3^+ \rightarrow 2^+$ Pt
$\gamma\gamma(\theta)$ Hamilton and Davies [a]	···	$-(10\pm1)$	$-(7.3^{+1.0}_{-0.8})$	···	···	$2.1^{+0.3}_{-0.2}$
$\gamma\gamma(\theta)$ Khan *et al.* [b]	···	<-4	$-(8\pm2)$	<-8 or >8	10^{+10}_{-3}	≈ 2
$\gamma\gamma(\theta)$ Grabowski [c]	···	$-(9.1^{+2.7}_{-1.7})$	$-(9.9\pm1.0)$	···	$10.9^{+2.1}_{-1.5}$	2.0 ± 0.2
$\gamma\gamma(\theta)$ Beraud *et al.* [d]	···	···	$-(6.3^{+0.6}_{-0.5})$	···	$7.6^{+1.6}_{-1.3}$	2.5 ± 0.2
$\gamma\gamma(\theta)$ Kenyon, *et al.* [e]	···	···	$-(9.4\pm1.5)$	<-11 or >11	···	3 ± 1
$\gamma(\theta,T)$ Reid *et al.* [f]	···	$-(15^{+10}_{-5})$	$-(7.3\pm0.2)$	<-1	~ 5	1.5 ± 0.1
$\gamma(\theta,T)$ present exp	$\delta^2 > 3.7$	$-(6^{+3}_{-1})$	$-(7.1\pm0.6)$	4^{+7}_{-3}	5.8 ± 0.8	1.5 ± 0.1
Calculated Kumar [g]	$\delta^2 = 30$	-14.8	-9.2	···	4.8	2.2

[a] See Ref. 3. [b] See Ref. 4. [c] See Ref. 5. [d] See Ref. 7.
[e] See Ref. 8. [f] See Ref. 11. [g] See Ref. 9.

By balancing λ^2/μ^2 and ν^2/μ^2, U_2 can be made equal to 0.850 even for large admixtures. At $\lambda^2/\mu^2 = 0.3$ (with $\nu^2/\mu^2 = 0.89$), U_4 is changed only by 6%. Moreover, the reported spectral shape[16] and β-γ correlation measurements are not seriously violated if the signs of λ/μ and ν/μ are suitably chosen. The present electron measurements will be seen to tighten this restriction.

The electron data were taken under widely varying circumstances, with variations in the results for different runs clearly beyond the apparent precision limits for each run. In some cases the magnetic saturation was clearly incomplete for the polarizing fields used; in others summing due to high fields distorted the spectra and produced a surplus of counts above the distinct 672-keV endpoint.

In all cases we consider energy bins centered at 416, 550, and 640 keV. These regions contained no major conversion-electron peaks. The numerous, identifiable peaks present elsewhere provided convenient energy markers; small gain changes were compensated for by choosing the same energy intervals for each counting period. The orientation parameters were again derived from the A_2 measured for the 468-keV γ ray.

The A_1 for the 672-keV β is measured positive; we will later deduce that B_1 is negative, but make use of that sign at this point in order to display R_1. In Table II the range of values that we measure for this quantity for the three energy intervals is shown. No average values or statistical error limits are given because the variations are not random but due to as yet incompletely explained differences in the experimental conditions.

This variation also conceals any true nonzero value for A_2; any limit that we could place would be less significant than that available from other experiments.

However, even the total range of R_2 for the 672-keV β and a limit of $|0.01|$ for the β-γ correlation coefficient magnitude[10] together produce a marked restriction on possible admixtures. In our approximation, for an electron energy of 560 keV,

$$R_1 = \frac{1.57\lambda\mu - 0.18\mu^2 - 1.22\nu\mu - 0.05\nu^2}{\lambda^2 + \mu^2 + 0.285\nu^2} .$$

If the transition is via pure tensor rank-one operators ($\lambda = \nu = 0$), the coefficient is clearly -0.18, agreeing with the observed magnitude of 0.11 to 0.28. The large interference terms, however, can easily dominate and even reverse the sign of the coefficient.

The previous discussion of the U_2 and U_4 restrictions showed that ν/μ would have to be appreciably larger than λ/μ. If we also invoke the β-γ anisotropy limitation, we find that for a simultaneous fit allowing large values of λ/μ and ν/μ each must be positive. This insures that R_1 is indeed negative and leads to the limits shown in Table III for the transition to the 4^+ level in platinum. The negative sign of B_1, taken with the known negative effective field for iridium in iron, yields a positive magnetic moment for the ^{192}Ir ground state.

In order to check for possible peculiarities in the 536-keV, $4^- \rightarrow 3^+\beta$ distribution as suggested,[10,17] we attempted to reproduce the R_1 coefficient measured in the 416-keV energy bin from calculated contributions from the 536- and 672-keV β groups. For pure tensor rank-one operators for each, the coefficients were, respectively, -0.835 and -0.177. Weighted with their respective spectral contributions at this energy, these yielded an average coefficient of -0.37, to be compared with the measured -0.212 to -0.307. However, this difference was not considered significant in view of the difficult experimental conditions. The measurement does not impose any further limitation on possible

B_{ij} contributions to the 536-keV transition.

The description of other transitions shown in Table III is determined from U_2 and U_4 results alone. The U_2 due to electron capture to the 580-keV level of ^{192}Os was characteristic of pure tensor rank-zero decay; the statistical limits for the weak 375-keV $E2$ γ ray would permit the indicated amount of impurities. Likewise the electron capture U_4 measured for the 485-keV γ ray indicated that little B_{ij} contribution could be possible for any δ. For the 240-keV β $4^- \rightarrow 4^+$ transition our results would correspond to about 20% tensor rank-zero contribution to a dominant tensor rank-one transition for no B_{ij} contribution. Additional amounts of both tensor rank zero and two cannot be ruled out.

We also analyzed the distribution of the K conversion electrons for the 468-keV transition; this R_2 also demonstrated variations greater than the 2 or 3% which counting statistics would have predicted for each run. Moreover, the R_2 displayed a most unlikely over-all dependence on the direction of the polarizing field. This effect did not depend strongly on the way peak areas and backgrounds were determined. The experimental particle parameter, A_2(conversion electron)/$A_2(\gamma)$, averaged 1.39 for P_1 positive and 2.19 for P_1 negative, while the theoretical value[18] is 1.33. This may be due to modulation by β summing, but is not quantitatively understood.

5. DISCUSSION

Hyperfine Interaction and Magnetic Moment

The supposition of constancy of an effective field for different states or isotopes of a given element can introduce considerable error. This has been explicitly shown to be true for two levels in ^{193}Ir, where the effective field for iridium in iron was found to differ by 7%.[19] For our determination of the orientation parameters we use the hyperfine interaction as directly measured. Moreover, B_2 is taken directly from the experimental data and should be applicable to all radiations independent of the hyperfine interaction. For B_1 and B_4, however, an error will occur if an interaction not appropriate to the circumstances is used.

TABLE II. Range of experimental β-distribution coefficients R_1.

Energy region (keV)	R_1 range
406 – 426	−0.212 to −0.307
541 – 578	−0.109 to −0.284
614 – 672	−0.145 to −0.308

For low external polarizing fields the hyperfine interaction we would have inferred from the measured foil temperature and the A_2 and A_4 for the 468-keV γ distribution was clearly too low. Conversely, for an H_{pol} of 2 kOe, a value of $\mu H = 1.3 \times 10^{-24}$ J fitted best. This is slightly larger than the reported value.[11]

The differences in response to external field were not studied in detail, but a possible cause would be a dependence on the iridium concentration. The conversion-electron peak-shape distortion would correspond to a penetration of greater than 0.1 mg/cm^2 of iron. This would indicate a concentration of less than 2 at.% if the iridium was uniformly distributed, in the case of the large-area sources. High local concentrations and the limited heat treatment used may have contributed to the field sensitivity.

In Ref. 11, their measurement of the magnitude of the magnetic moment is compared with values predicted for certain spherical and slightly deformed ground-state configurations for ^{192}Ir. For a $d_{3/2}$-proton, $f_{5/2}$-neutron basic configuration both give a positive magnetic moment, in agreement with the sign determined in the present experiment.

$E2/M1$ Mixing Ratios

The agreement in γ mixing ratios shown in Table I in general is quite good, both among the various experimental values and their average compared with the theoretical, based on the comprehensive calculations of Kumar and Baranger[20] using a pairing-plus-quadrupole microscopic model.

The small difference between the nuclear orientation and γ-γ correlation results for the accurately measured 604-keV transition might be attributed to error in accounting for the orientation or repopulation factors in the former, but there is no consistent discrepancy for the 308-keV transition arising from the same 921-keV level. Likewise, any unlikely attenuation from perturbations in the 50-psec 316-keV level which could reduce this γ-γ anisotropy should affect the 296-keV result. Also, measurements of the 468–316-keV $4^+ \rightarrow 2^+ \rightarrow 0^+$ cascade showed no attenuation.[5] The value of 1.5

TABLE III. Relative contributions of operators of tensor rank 0, 1, and 2 in each of four transitions from the ground state of ^{192}Ir.

	Electron capture to ^{192}Os			Electron emission to ^{192}Pt		
Transition	0	1	2	0	1	2
$4^- \rightarrow 4^+$	~1	<0.4	<0.1	<0.08	~1	<0.03
$\rightarrow 3^+$	···	~1	<0.1	···	~1	<0.2

for the δ of the 604 transition would lead to a K conversion coefficient of 2.02×10^{-2}, in good agreement with the experimental value of $(2.01\pm0.07)\times10^{-2}$, using the same input information that Grabowski[5] used to predict a value of $(1.75^{+0.10}_{-0.07})\times10^{-2}$ for a δ of 2.0 ± 0.2.

The weaker γ rays do not permit comparisons of very great accuracy, but in no case is a large $M1$ contribution calculated or found. The 417-keV γ originates from a second 4^+ state not included in the calculations used for comparison.

For the β transitions no theoretical calculations yet exist, but it is clear that both the logft values and the relative contribution of different operators differ for the electron capture and β decays to states of the same spin. The β transition to the lower 4^+ state is essentially all by tensor rank-one operators; the corresponding electron-capture transition is compatible with all tensor rank zero. The transition to the upper 4^+ platinum state also contains definite tensor rank-zero contributions. In no case is any positive evidence for a tensor rank-two component found.

At this point no evidence remains for any cancellations in the β decay. The recent evidence against any β-γ anisotropy[17] suggests that any more detailed study of the β distributions directed toward an identification of the individual matrix elements would probably not be justified. In fact, the only experimental evidence that the decays are not allowed is the somewhat large ft values.

Our present experience indicates that good-resolution electron spectroscopy with oriented nuclei is possible, but that further investigation is necessary before the full inherent accuracy can be utilized.

6. ACKNOWLEDGMENTS

We wish to thank John Twomey and Dr. Francis Schima for their assistance with the experiment. We are also indebted to the radioactivity and neutron physics sections for the use of equipment.

[1]L. Schellenberg, O. Huber, P. Siffert, and J. M. Kuchly, Helv. Phys. Acta 40, 639 (1967).

[2]T. J. Palaska, V. R. Potnis, and C. E. Mandeville, Nucl. Phys. A95, 673 (1967).

[3]W. D. Hamilton and K. E. Davies, Nucl. Phys. A122, 165 (1968).

[4]M. Y. Khan, L. D. Wyly, C. H. Braden, and E. T. Patronis, Jr., Phys. Rev. 182, 1259 (1969).

[5]Z. W. Grabowski, Phys. Rev. 1[illegible] 1019 (1969).

[6]M. Levanoni, Phys. Rev. 186, 1253 (1969).

[7]R. Béraud, I. Berkes, R. Chéry, R. Haroutunian, M. Lévy, G. Marguier, G. Marest, and R. Rougny, Phys. Rev. C 1, 303 (1970).

[8]D. B. Kenyon, L. Keszthelyi, and J. A. Cameron, Can. J. Phys. 47, 2395 (1969).

[9]K. Kumar, Phys. Letters 29B, 25 (1969).

[10]S. K. Bhattacherjee, S. K. Mitra, H. C. Jain, and H. C. Padhi, Phys. Rev. 159, 1056 (1967).

[11]P. G. E. Reid, M. Sott, and N. J. Stone, Nucl. Phys. A129, 273 (1969).

[12]H. J. Rose and D. M. Brink, Rev. Mod. Phys. 39, 306 (1967).

[13]M. Morita and R. S. Morita, Phys. Rev. 109, 2048 (1958).

[14]A. V. Kogan, V. D. Kul'kov, L. P. Nikitin, N. M. Reĭnov, M. F. Stel'makh, and M. Schott, Zh. Eksperim. i Teor. Fiz. 43, 828 (1962) [transl.: Soviet Phys. – JETP 16, 586 (1963)].

[15]J. A. Cameron, I. A. Campbell, J. P. Compton, R. A. G. Lines, and N. J. Stone, Nucl. Phys. 59, 475 (1964).

[16]M. W. Johns and M. Kawamura, Nucl. Phys. 61, 385 (1965).

[17]This β-γ anisotropy has now been shown by the authors to be due to unresolved conversion electrons. See S. K. Bhattacherjee and H. C. Jain, Bull. Am. Phys. Soc. 14, 1226 (1969).

[18]*Alpha-, Beta-, and Gamma-Ray Spectroscopy*, edited by K. Siegbahn (North-Holland Publishing Company, Amsterdam, The Netherlands, 1965), Appendix 7.

[19]G. J. Perlow, W. Henning, D. Olson, and G. L. Goodman, Phys. Rev. Letters 23, 680 (1969).

[20]K. Kumar and M. Baranger, Phys. Rev. Letters 17, 1146 (1966); Nucl. Phys. A122, 273 (1968).